BJR, 2026, **99**, 65–72
https://doi.org/10.1093/bjr/tqaf219
Advance access publication: 28 August 2025
Research Article

Not all tumors are alike: varying efficacy of FLASH across tumor types and oxygenation status in spheroid models

Rebecka Dela, MD[1], Liliana Lemos Da Silva, PhD[2], Sarah Beyer, MSc[1], Brita Singers Sørensen, PhD[3], Per Poulsen, PhD[3], Elise Konradsson, PhD[2], Filip Hörberger, MSc[2], Kristoffer Petersson, PhD[4,5], Crister Ceberg, PhD[2], Gabriel Adrian, MD, PhD[1,5,*]

[1]Division of Oncology and Pathology, Department of Clinical Sciences, Lund University, Lund, 22242, Sweden
[2]Department of Clinical Sciences, Medical Radiation Physics, Lund University, Lund, 22242, Sweden
[3]Danish Centre for Particle Therapy, Aarhus University Hospital, Aarhus, 8200, Denmark
[4]Department of Oncology, Oxford Institute for Radiation Oncology, University of Oxford, Oxford, OX3 7DQ, United Kingdom
[5]Department of Hematology, Oncology and Radiation Physics, Skåne University Hospital, Lund, 22242, Sweden

*Corresponding author: Gabriel Adrian, MD, PhD, Division of Oncology and Pathology, Department of Clinical Sciences, Lund University, Barngatan 4, Lund 22242, Sweden (gabriel.adrian@med.lu.se)

Abstract

Objectives: Ultra-high dose rate irradiation (UHDR) has been shown to spare normal tissue in various model systems. This study evaluates its potential to sterilize cancer cells using spheroid tumor models.

Methods: Spheroids from glioblastoma (U87), hypopharyngeal squamous cell carcinoma (2 sizes, $FaDu_{small}$ and $FaDu_{large}$) and breast adenocarcinoma (T47D) cells were irradiated with electron beams using UHDR (>200 Gy/s) or conventional dose rate (CONV, ∼0.1 Gy/s) exposures under ambient or reduced oxygen (1%) conditions. U87 and $FaDu_{small}$ were also irradiated with protons. Spheroids were monitored using imaging for up to 100 days to determine the dose required to cure 50% of spheroids (SCD_{50}). These data were used to calculate dose-modifying factor estimates for UHDR at the 50% survival level (DMF_{SCD50}).

Results: A total of 3230 spheroids were analyzed. Under ambient oxygen tension, UHDR and CONV showed no significant differences in U87 ($DMF_{SCD50} = 0.98$, $P = .47$), $FaDu_{small}$ ($DMF_{SCD50} = 1.01$, $P = .75$), and T47D ($DMF_{SCD50} = 1.04$, $P = .25$), regardless of electron or proton irradiation. Under reduced oxygen levels, significantly higher UHDR doses were required to sterilize the spheroids, with DMF_{SCD50} 1.14 (U87, $P < .01$), 1.07 ($FaDu_{small}$, $P = .02$), and 1.13 (T47D, $P < .01$). $FaDu_{large}$-spheroids irradiated under ambient oxygen showed a DMF_{SCD50} of 1.66 ($P < .001$).

Conclusion: Using spheroid tumor models with long follow-up, we demonstrate that efficacy of UHDR varies across cancer types and conditions. Whereas small spheroids exhibit iso-efficacy, both reduced oxygen tension and increased spheroid size lead to higher DMF.

Advances in knowledge: This preclinical study suggests that tumor iso-efficacy with UHDR may not hold true for all cancer types and is associated with oxygen level.

Keywords: ultra-high dose rate irradiation; FLASH; tumor control; preclinical models; hypoxia; spheroids.

Introduction

Over the past decade, ultra-high dose rate irradiation (UHDR) has been demonstrated to preferentially increase tolerance in normal tissues. It has been shown for tissues such as skin, brain, intestines, and lung, offering hope to reduce the dose-limiting side effects associated with clinical radiotherapy.[1-4] In a recent comprehensive analysis of published literature on tumor efficacy, it was found that on average, no differences in tumor responses could be seen between UHDR and conventional dose rate irradiation (CONV).[5] Thereby, UHDR should provide a widening of the therapeutic window, which is known as the FLASH effect. However, the studies assessing tumor efficacy were found to be mostly relying on tumor growth comparisons between UHDR and CONV at 1 or a few dose levels with a short follow-up (average 30 days), potentially hampering the ability to detect smaller dose-rate dependent differences. Only 1 study provided results from a tumor controlling dose (TCD_{50}) experiment.[6]

According to classical radiobiological target theory, a tumor is sterilized when every clonogenic cell is killed.[7] To assess the curative potential *in vivo*, the golden standard is to use TCD_{50}-experiments with long enough follow-up to allow surviving cells to repopulate the tumor.[8,9] In earlier days of radiobiological research, studies utilizing thousands of mice were used, providing detailed tumor-response relationships.[10,11] With the current views of animal ethics in research, such experiments might be hard to justify, and would also come at a considerable cost.[12,13] Nonetheless, when investigating a new radiation technique such as UHDR, it is of utmost importance to comprehensively investigate its potential to sterilize cancer cells in preclinical models.

There are several open questions in our current knowledge of the FLASH effect. The underlying mechanism is to be elucidated, as well as the differential effect seen on tumors compared with normal tissue. Moreover, it is not known if all tumors, or tumors in different environments, respond in a similar way following UHDR or CONV irradiation. The role of oxygen has been widely investigated and debated, and different experiments have found contradictory results with increased or decreased effect of UHDR in hypoxia.[14-19] Some

Received: 22 May 2025; **Revised:** 30 July 2025; **Accepted:** 20 August 2025

studies suggest a dose-threshold before a FLASH-effect can be seen, whereas other experiments report FLASH-effects occurring at doses well below 10 Gy.[20-22]

In this study, UHDR irradiation was administered using electron or proton beams, which are currently the predominant methods, whereas photon-based UHDR remains technically challenging.[23] Each method has its advantages, and only few studies have compared electron and proton UHDR within the same model system.[24-26]

To allow a detailed assessment of tumor response after UHDR, we have established a spheroid tumor model allowing large-scale experiments with long follow-up. While still being *in vitro*, the 3D-structure of the spheroids contributes to a naturally occurring oxygen and nutrient gradient, as well as cell-to-cell-interactions.[27,28] The aim of the present study was to comprehensively evaluate the potential of UHDR to sterilize cancer cells using spheroid tumor models, addressing the following questions:

1) is the sterilization efficacy maintained across different cancer cell lines?
2) is the sterilization efficacy affected by variations in conditions such as oxygen levels and spheroid size?

Methods

Spheroid models

To study responses across different cancer types, we selected 3 cell lines representing tumors where radiotherapy plays a key role in the clinical management. The hypopharyngeal squamous cell carcinoma cell line FaDu (ATCC:HTB-43) was acquired from DSZS (DSZS German Collection of Microorganisms and Cell Cultures GmbH, Braunschweig, Germany). The hormone receptor positive breast adenocarcinoma cell line T47D (ATCC:HTB-133) and the glioblastoma cell line U87 (ATCC:HTB-14) were acquired from ATCC (Manassas, VA, USA). Exponentially growing cells were grown in DMEM (Sigma-Aldrich, Schnelldorf, Germany) supplied with 10% fetal bovine serum (FBS) and 1% penicillin-streptomycin (PEST, Sigma-Aldrich, Schnelldorf, Germany) and maintained in a humidified incubator at 37°C and 5% CO_2.

Spheroids were constructed by using non-adherent specially coated U-shaped 96-well plates (Cat No 7007, Corning, Tewksbury, MA, USA). For the $FaDu_{large}$ spheroids, 50 000 cells were used, while 5000 cells were used for the $FaDu_{small}$, and for the T47D and U87 spheroids. The specified number of cells were added per well, and the plates were placed on an orbital shaker set to 100 rpm in an incubator for 2-3 days to allow spheroids to form. Throughout the experiments, the cell medium was carefully exchanged twice weekly, with half of the volume being replaced each time. The size of the spheroids was assessed by high-resolution scanning. The spheroids were monitored for up to at 100 days after irradiation, or, for some samples, until they had clearly surpassed the volume thresholds and were thereby considered treatment failures. For further details, see Supplementary Methods.

Irradiation

Electron beam irradiations were performed on a modified Elekta Precise (Elekta AB, Stockholm, Sweden) medical linear accelerator at an energy of 10 MeV allowing irradiation at dose rates up to ultra-high values as previously described.[29,30] Proton irradiation was performed using pencil beam scanning (PBS) on the fixed horizontal beam line at Danish Centre for Particle Therapy at Aarhus University Hospital, Denmark.[31] For details, see Table 1 for beam characteristics and Supplementary Methods.

Table 1. Beam characteristics for ultra-high dose rate and conventional dose rate irradiation, using electrons and protons.

	CONV	UHDR
Irradiation type	Electrons	Electrons
Beam energy	10 MeV	10 MeV
Dose per pulse	0.65 mGy	1.0 Gy
Pulse repetition frequency	200 Hz	200 Hz
Pulse width	3.5 µs	3.5 µs
Minimum dose rate for any dose	0.13 Gy/s	200 Gy/s
	CONV	**UHDR**
Irradiation type	Protons	Protons
Beam energy	244 MeV	250 MeV
Field size (mm^2)	24 × 80	24 × 80
No. of spots	7 × 21	7 × 21
Spot spacing (mm)	4	4
Repaintings	37× to 120×	None
Field dose rate (Gy/s)	0.24 ± 0.02	24.8 ±1.6
Pencil Beam Scanning dose rate (Gy/s)	0.24 ± 0.02	161 ± 21

Hypoxia

To reduce the level of available oxygen, we used a hypoxia chamber (HypoxyLab, Oxford Optronix, Adderbury, UK) set to 8 mmHg oxygen tension (~1.1%), 37°C, 70% humidity, and 5% CO_2. Spheroids subject to hypoxia were placed in the hypoxia chamber 24 hours prior to irradiation. While remaining in the hypoxia chamber, a sterile seal tape (SealPlate Film, Sigma-Aldrich, St. Louis, MO, USA) was tightly applied to maintain the reduced oxygen state during irradiation. Following irradiation, the plates were put back in the hypoxia chamber, the seal was removed, and incubated for another 24 hours under reduced oxygen tension before being moved to an incubator set to ambient oxygen level. Hypoxia within spheroids was visualized using immunofluorescence staining of GLUT1 (Supplementary Methods).

Data analysis and statistics

Sterilization of spheroids was determined by the end of follow-up, with at least 12 spheroids analyzed per condition and dose level. The dose-response relationship was fitted using logit analysis, which was also used to estimate the spheroid controlling dose to sterilize 50% of the spheroids, SCD_{50}. To incorporate the time component of the radiation response, additional analyses of time-to-reach 5× the initial volume (TGT $5V_0$) was analyzed using Cox-regression with all dose levels and dose rate (UHDR *vs.* CONV) within a single statistical model. For details, see Supplementary Methods.

Results

In total, 3230 spheroids (598 U87, 432 T47D, 884 $FaDu_{small}$, and 1316 $FaDu_{large}$ spheroids) were treated and followed for up to 100 days in experiments conducted over a period of 2 years. All spheroid models showed clear dose-response relationship, but with distinct growth and response characteristics. U87-spheroids grew directly upon seeding, and following irradiation, the spheroids continued to grow

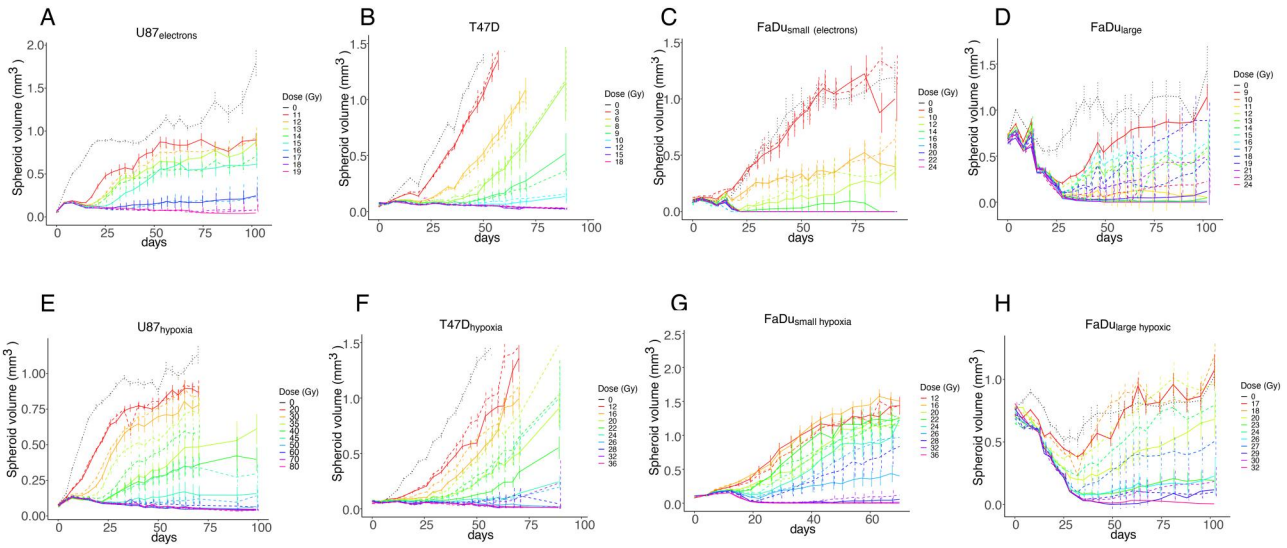

Figure 1. Spheroid growth curves displaying the evolution up to 100 days after irradiation for the glioblastoma U87 (A and E), breast adenocarcinoma T47D (B and F), squamous cell carcinoma $FaDu_{small}$ (C and G), and $FaDu_{large}$ (D and H), after electron irradiation in ambient oxygen tension (A-D) or under reduced oxygen (1.1%) (E-H) at conventional dose-rate (CONV, solid lines) or UHDR (dashed lines), and non-irradiated controls (dotted lines). Colors indicate the irradiation doses as noted in the figure legends, and vertical lines display 1 SE of the volumes at the indicated time point.

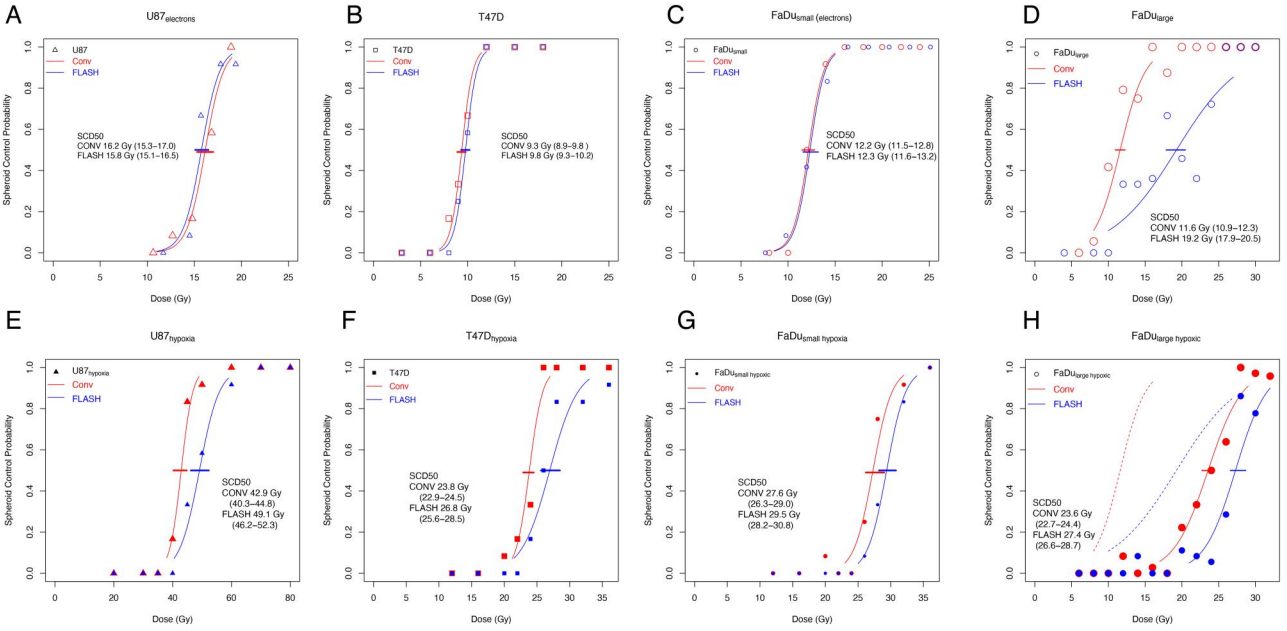

Figure 2. Spheroid controlling probability as a function of dose for U87 (A and E), T47D (B and F), $FaDu_{small}$ (C and G), and $FaDu_{large}$ (D and H), after electron irradiation in ambient oxygen tension (A-D) or under reduced oxygen (1.1%) (E-H). Markers represent the proportion of spheroids cured at the indicated dose, for CONV (red) and UHDR (blue), as well as the fitted regression lines. The spheroid controlling dose (SCD_{50}) indicate the dose required to sterilize 50% of the spheroids, with 95% confidence interval in brackets.

for 5-7 days before responding with a dose-dependent growth-delay. T47D-spheroids started to grow about a week after seeding, and displayed a substantially longer growth-delay following irradiation compared with U87. $FaDu_{small}$ spheroids started to grow 2-3 weeks upon seeding. $FaDu_{large}$-spheroids shrunk in size during the first 3-4 weeks while forming a dense core, followed by a growth period, just surpassing the initial volume.

Spheroids displaying iso-efficacy to UHDR radiation

The U87, T47D, and $FaDu_{small}$-spheroids all demonstrated similar responses to UHDR and CONV irradiation in ambient conditions (Figure 1A-C). No significant differences in sterilizing efficacy were observed between the 2 modalities, as indicated by overlapping SCD_{50}-values and DMF_{SCD50} estimates not significantly different from 1 (Figure 2A-C and Table 2). Likewise, the Cox-regression analysis revealed no dose rate-dependent difference in growth, with DMF_{Growth} estimates also not significantly different from 1 (Table 3).

The response to proton irradiation was investigated in U87- and $FaDu_{small}$-spheroids. The growth behavior was similar for proton-UHDR and proton-CONV (Figure 3A and B) with no difference in statistical testing using Cox-regression (Table 3). There was no difference in the sterilizing efficacy

Table 2. Summary of estimated spheroids controlling doses (SCD_{50}) to sterilize 50% of the spheroids for CONV and UHDR across the spheroids studied, with corresponding 95%CI.

Cell line	Condition	Irradiation	$SCD50_{CONV}$	95% CI	$SCD50_{FLASH}$	95% CI	*P* (FLASH *vs.* CONV)	DMF_{SCD50}	95% CI
U87	Normoxic	Electron	16.2	15.3-17.0	15.8	15.1-16.5	.47	0.98	0.91-1.04
U87	Hypoxic	Electron	42.9	40.3-44.8	49.1	46.2-52.3	<.01	1.14	1.07-1.22
T47D	Normoxic	Electron	9.3	8.9-9.8	9.8	9.3-10.2	.25	1.04	0.98-1.12
T47D	Hypoxic	Electron	23.8	22.9-24.5	26.8	25.6-28.5	<.01	1.13	1.08-1.17
$FaDu_{small}$	Normoxic	Electron	12.2	11.5-12.8	12.3	11.6-13.2	.75	1.01	0.94-1.11
$FaDu_{small}$	Hypoxic	Electron	27.6	26.3-29.0	29.5	28.2-30.8	.02	1.07	1.01-1.14
$FaDu_{large}$	Normoxic	Electron	11.6	10.9-12.3	19.2	17.9-20.5	<.001	1.66	1.54-1.83
$FaDu_{large}$	Hypoxic	Electron	23.6	22.7-24.4	27.4	26.6-28.7	<.001	1.16	1.10-1.21
U87	Normoxic	Proton	18.6	18.0-19.4	18.6	18.0-19.3	.87	1.00	0.95-1.05
$FaDu_{small}$	Normoxic	Proton	13.6	13.3-14.0	13.9	13.6-14.2	.24	1.02	0.99-1.05

The dose modifying factor (DMF_{SCD50}) at the SCD_{50} dose level is presented, with values greater than 1 indicate reduced efficacy of UHDR compared to CONV.

Table 3. Analyses of time to reach 5× the initial volume ($5V_0$) using a Cox-regression model, providing β-estimates for the covariates dose and dose rate (coded as 1 for UHDR and 0 for CONV).

Cell line	Condition	Irradiation	β_{FLASH}	*P*	β_{Dose}	*P*	$\beta_{interaction}$	*P*	DMF_{Growth} at SCD50 (95%CI)
U87	Normoxia	electron	−.201	.42	−.682	<.001		NS	0.98 (0.93-1.03)
U87	Hypoxia	electron	−1.029	.28	−.388	<.001	.073	.014	1.13 (1.08-1.17)
T47D	Normoxia	electron	.032	.89	−1.219	<.001		NS	1.00 (0.96-1.04)
T47D	Hypoxia	electron	1.249	<.001	−.449	<.001		NS	1.12 (1.06-1.17)
$FaDu_{small}$	Normoxia	electron	.007	.98	−.627	<.001		NS	1.00 (0.93-1.07)
$FaDu_{small}$	Hypoxia	electron	−1.275	.022	−.232	<.001	.0684	0.010	1.10 (1.03-1.15)
U87	Normoxia	proton	.03	.61	−.673	<.001		NS	1.00 (0.97-1.03)
$FaDu_{small}$	Normoxia	proton	−.217	.07	−.438	<.001		NS	0.96 (0.92-1.00)

A statistical interaction term between dose and dose rate was examined to assess potential dose-dependent differences in efficacy. When significant, the interaction term was included in the model. The β-estimates were used to calculate corresponding dose-modifying factor (DMF_{Growth}) for UHDR *versus* CONV at the SCD_{50}-dose. For further details, see the Supplementary Material. NS: Not significant.

for the proton-irradiated U87- and $FaDu_{small}$-spheroids in ambient conditions (Figure 3C and D and Table 2).

UHDR response with varying oxygen level and spheroid size

We next aimed to investigate the UHDR response under varying conditions, by altering spheroid size and inducing hypoxia by reducing the available oxygen.

As expected, reducing oxygen induced a significant radioresistance across all spheroid models. On average, a 2.5× higher dose was required to sterilize 50% of the hypoxic spheroids using CONV-irradiation. $U87_{hypoxic}$ demonstrated a sparing with SCD_{50}-doses of 49.1 Gy (46.2-52.3) for UHDR compared with 42.9 Gy (40.3-44.8) for CONV ($P <$ .01), representing a DMF_{SCD50} of 1.14 (1.07-1.22) (Figure 2E and Table 2). The growth analyses revealed a significant interaction ($P = .01$) between dose and dose rate, representing larger sparing for UHDR with increasing dose. At the SCD_{50}-dose a DMF_{Growth} of 1.13 (1.08-1.17) was estimated (Table 3). For $T47D_{hypoxic}$ the SCD_{50}-doses were 26.8 Gy (25.6-28.5) and 23.8 Gy (22.9-24.5) for UHDR and CONV, respectively ($P <$ .01), representing a DMF_{SCD50} 1.13 (1.06-1.21) (Figure 2F and Table 2). This was also reflected in the growth analyses with a DMF_{Growth} of 1.12 (1.06-1.17) (Table 3 and Figure S1). For $FaDu_{small\ hypoxic}$ the SCD_{50}-doses were 29.5 Gy (28.2-30.8) and 27.6 Gy (26.3-29.0) for UHDR and CONV, respectively ($P = .02$), representing a modest DMF_{SCD50} of 1.07 (1.01-1.14) (Figure 2G). Again, the growth analyses revealed a significant interaction, suggesting less efficacy for UHDR with increasing dose ($P = .01$) and an estimated DMF_{Growth} of 1.10 (1.03-1.15) at the SCD_{50}-dose (Table 3).

The FaDu cell line was further examined by increasing the spheroid size. These $FaDu_{large}$-spheroids showed a different response compared to the $FaDu_{small}$-spheroids. Following CONV-irradiation, a typical dose-response relationship was observed, with a SCD_{50} of 11.6 Gy (10.9-12.3). In contrast, UHDR-irradiation produced an indistinct dose-response relationship in the 12-22 Gy dose-range (Figures 1D and 2D). A significant sparing was found, with SCD_{50} of 19.2 Gy (17.9-20.5, $P <$ .001 compared with CONV), representing a large DMF_{SCD50} of 1.66 (1.54-1.83).

Additionally, $FaDu_{large}$-spheroids were investigated under reduced oxygen conditions. In these $FaDu_{large\ hypoxic}$, the sparing was less pronounced compared with ambient conditions, although it remained significant with SCD_{50} of 27.4 Gy (26.6-28.7) for UHDR compared with 23.6 Gy (22.7-24.4) for CONV ($P <$ .001), representing a DMF_{SCD50} of 1.16 (1.10-1.21). Moreover, the indistinct dose-response relationship found for UHDR in $FaDu_{large}$ was not present under reduced oxygen conditions, and the steepness of the curve for UHDR resembled the one for CONV (Figure 2H).

Immunofluorescence to visualize hypoxia

A small core of cells expressing hypoxic marker GLUT1 was present in the center of the $FaDu_{small}$-spheroids, while the outer layers showed no signs of hypoxia (Figure 4A). Hypoxia treatment for 24 hours efficiently upregulated hypoxic markers throughout all cell layers (Figure 4E). In the $FaDu_{large}$, a large proportion of the cells were spontaneously

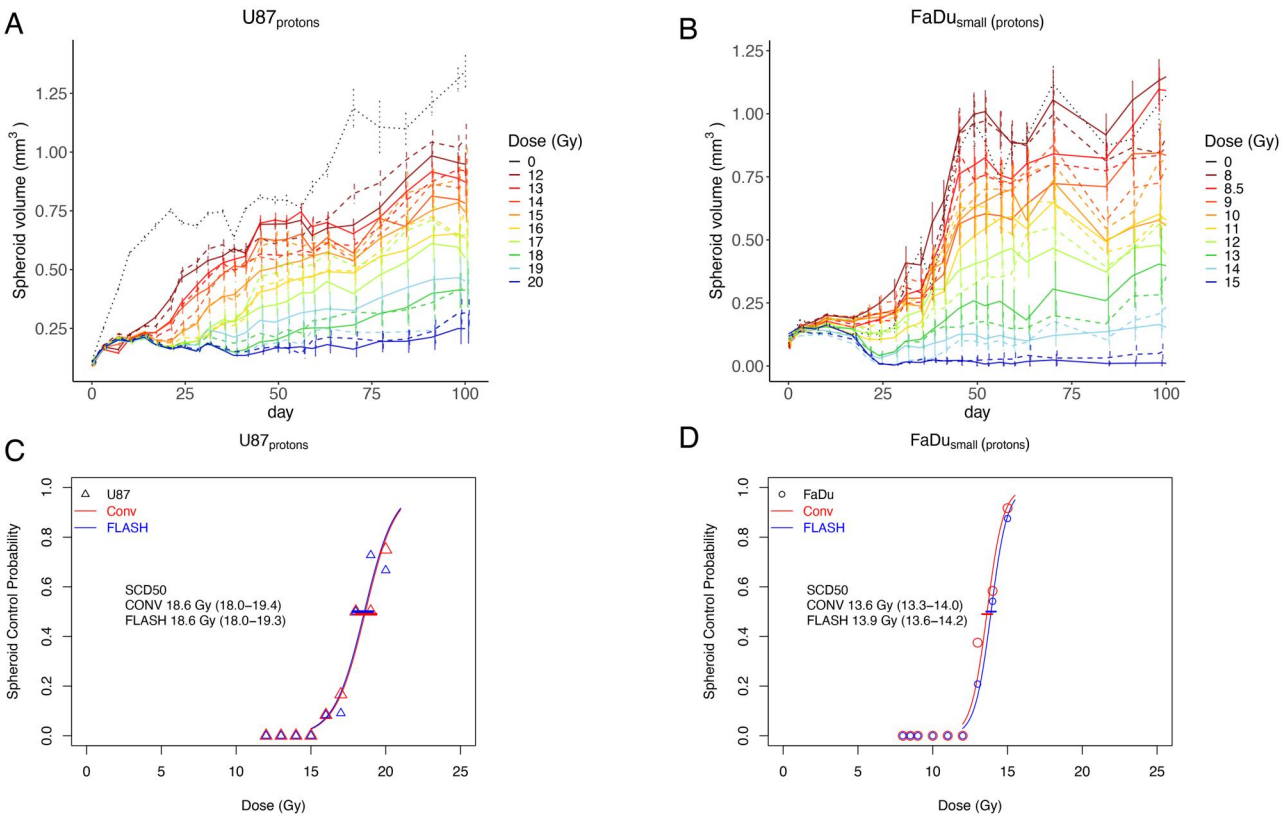

Figure 3. Spheroid growth curves for U87 (A) and $FaDu_{small}$ (B) treated with proton irradiation under ambient oxygen tension at conventional dose-rate (CONV, solid lines) or UHDR (dashed lines), and non-irradiated controls (dotted lines). Colors indicate the irradiation doses as noted in the figure legends, and vertical lines display 1 SE of the volumes at the indicated time point. (C, D) Corresponding tumor spheroid controlling probability for U87 (C) and $FaDu_{small}$ (D).

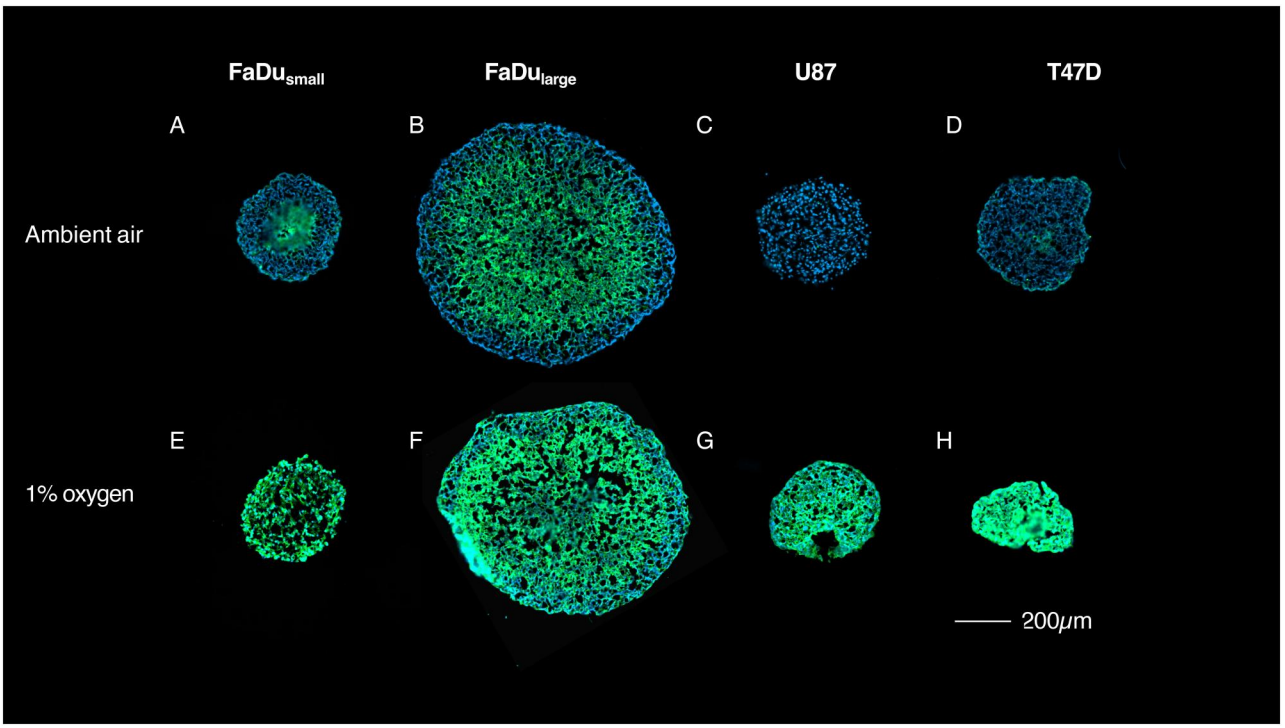

Figure 4. Immunofluorescence staining of 3-day-old spheroids for endogenous hypoxia expression using GLUT1 (green), with cell nuclei counterstained using Hoechst (blue). Spheroids were incubated under ambient oxygen conditions ($FaDu_{small}$ (A), $FaDu_{large}$ (B), U87 (C), and T47D (D)), or under reduced oxygen tension (1.1%) for 24 hours prior to imaging ($FaDu_{small}$ (E), $FaDu_{large}$ (F), U87 (G), and T47D (H)). Scale bar indicates the magnification.

expressing hypoxic markers, excluding the outermost cell layers. (Figure 4B). Hypoxia treatment upregulated GLUT1-expression throughout the spheroids (Figure 4F).

In the U87- and T47D spheroids, no hypoxic staining were displayed in ambient conditions (Figure 4C and D), but heavily upregulated after hypoxic treatment (Figure 4G-H).

Discussion

We have used an *in vitro* model allowing large-scale experiments with high statistical power to study responses after UHDR irradiation. The results reveal that spheroid tumor models do not respond uniformly to UHDR. Whereas some spheroids are equally efficiently controlled by UHDR as CONV, others exhibit a significant sparing effect. The sparing occurred across different histological subtypes and was affected by spheroid size and oxygen tension, with a clear sparing effect for larger spheroids or hypoxic conditions.

The spheroid model provided a detailed dose-response relationship. In the present *in vitro* attempts to mimic tumor cure, the model provides radiobiologically relevant results that reflect the survival of clonogenic cells, consistent with classical target theory. The long follow-up should allow enough time for a few, or even a single, surviving cell to divide and repopulate the tumor. Thereby, the model is useful to investigate potential differences in tumor response between UHDR and CONV. Accordingly, the study detected statistically significant results corresponding to less than a 10% difference in DMF_{SCD50}. Such a small magnitude of difference could easily go undetected in *in vivo* models using 10 animals per condition, at a single dose level.

A sparing effect at UHDR is widely shown to occur in normal tissues.[1-3,20,32-35] The present results show that a sparing can also arise in tumor models, with dose-modifying factors of 1.07-1.66, which is similar to observations for normal tissues. Interestingly, the sparing effect differed and was most pronounced in the large $FaDu_{large}$-spheroids under ambient oxygen tension, whereas iso-efficacy between UHDR and CONV was found in small spheroids from the same cell line. Thereby, the present sparing should not be defined by genetics or histology. Instead, phenotypic changes that arise in the $FaDu_{large}$-spheroids appear to trigger the sparing effect. Here, oxygen tension, nutrient gradients, altered cell-cell-interaction, cell cycle distributions, and necrotic areas could play a role. Importantly, reduction in available oxygen (24 hours before and after irradiation) altered the UHDR response in the spheroid types studied. In the U87-, T47D-, and the $FaDu_{small}$-spheroids, reduced oxygen induced a sparing effect. For $FaDu_{large}$, a sparing effect persisted under reduced external oxygen conditions, though it was less pronounced than under ambient conditions.

The spatial distribution of hypoxia, as assessed by immunofluorescence staining of endogenous marker, differed between the spheroids studied. Thereby, the current results picture an intricate relationship between oxygen, tumor-specific factors and response to UHDR. While not ruling out a tumor-agnostic first-order relationship between UHDR response and oxygen, a more detailed understanding of currently unknown tumor-specific factors is needed. Baseline oxygen tension, nutrient gradients, and cell cycle differences are known to be dependent on spheroid size, and differ between tumor types.[27,36] For the spheroid models used in this study, size-dependent oxygen gradients, oxygen consumption and thresholds for expressing endogenous GLUT1 might have impacted the hypoxia stainings. However, it was evident that lowering the oxygen level effectively induced the expression across cancer types. It could also be noted that despite expression of hypoxic markers in the core of $FaDu_{small}$-spheroids (Figure 4A), no sparing effect was found at UHDR.

We have previously found a sparing effect at UHDR *in vitro* using 2D-monolayer clonogenic assays.[22] Similar to the present results, an oxygen dependance was evident in that model as well.[19] The present spheroid model has several advantages compared to traditional 2D-monolayer clonogenic assays. Like *in vivo* studies, there is no initial difference between spheroids across the different dose levels. In clonogenic assays, the number of seeded cells typically differs, which has been shown to affect the radiation response.[37] The spheroid model allows for a wider dose-range to be studied, whereas clonogenic assays provide challenges at higher dose levels with low surviving fractions.[38,39] It is also plausible to assume that the intramodel variety, such as proliferative status and cell cycle-phases across cells, are more heterogenous in spheroids compared to clonogenic assays, which should resemble the *in vivo* scenario to a higher degree.[27] Moreover, the long follow-up time used in the spheroid model provides additional information, as some spheroids started to grow more than 2 months after irradiation.

To our knowledge, there are no published *in vivo* studies reporting a sparing effect of tumors. Instead, iso-efficacy, or even enhanced tumor efficacy, have been reported.[1-3,6,21,32,40-48] The only published TCD_{50}-study investigating UHDR found iso-efficacy for the C3H-breast cancer model, subcutaneously grown on the foot of the mice.[6] There are, however, previous *in vitro* findings where UHDR was less efficient compared with CONV. Using clonogenic assays, reduced efficacy of UHDR was found under ambient conditions,[2,22] whereas oxygen-dependent differences were found in other studies.[19,49] Moreover, tumors in *in vivo* models typically exhibit hypoxia,[50] although no apparent sparing at UHDR has been published to date. These discrepancies will be crucial to investigate in future studies. In this regard, it should be noted that most *in vivo* results are based on small studies with short follow-up using tumor growth as primary endpoint. From previous studies it is known that tumor growth-based endpoints do not always correlate with TCD_{50}-assays, with the latter one being regarded as the golden standard.[9,51-53] Based on the current results, further *in vivo* studies using TCD_{50}-assays and a variety of cancer models under different conditions seem indicated.

Using the same proton beam as Sørensen et al,[6] the current results for the U87 and $FaDu_{small}$-spheroids are well in line with previous *in vivo* data indicating iso-efficacy. Adding to this, we used the same spheroid model for electron- and proton-irradiation, both providing iso-efficacy between CONV and UHDR. For practical reasons hypoxic conditions could not be investigated by protons in this study, but this would be interesting to address in coming studies to see if the observed sparing effect also applies for other beam modalities than pulsed electron beams. There still may be differences in response between the modalities. Beam characteristics, such as scanning mode, pulse dose-rate, pulse repetition frequency and dose per pulse, total irradiation time, innately differs between electron and proton-UHDR. The importance of beam characteristics in the UHDR field is an ongoing area of research.[54]

Previous data suggest that sparing at UHDR becomes more evident at higher doses.[20] In this study, the statistically

significant interaction between dose and dose rate in the growth analyses ($U87_{hypoxia}$ and $FaDu_{hypoxia}$) suggests a potential relationship between sparing effect and dose level. However, our results do not support the existence of a universal dose-threshold for sparing, as U87 exhibited iso-efficacy at higher doses than those at which sparing occurred for $FaDu_{large}$. Further studies with additional data are needed to clarify the nature of this association.

Spheroid models have previously been shown to resolve a sparing effect at UHDR. Khan et al[49] irradiated spheroids, dissolved them, reseeded for clonogenic survival, and showed a sparing effect for lung cancer A549 cells. DNA damages in spheroids were recently demonstrated to be reduced after UHDR for certain conditions.[55] The present results further add to these findings and demonstrate a varying efficacy of UHDR depending on oxygen tension and spheroid size.

The clinical implications of the current findings remain to be investigated. While UHDR could provide efficacious eradication of certain tumors, there is a prudent risk that others may be spared. It is outside the scope of the present paper to speculate which clinical scenarios (eg, radical treatment *vs.* adjuvant treatment for microscopic disease), tumor characteristics, histologies or phenotypes that are, or are not, suitable for UHDR. But we believe that the results underline that clinical trials should be preceded with rigorous preclinical testing, to carefully select appropriate tumors and clinical scenarios for UHDR trials.

There are several limitations in this study. Using a purely *in vitro* based model, the results do not necessarily reflect the *in vivo* response to UHDR. There is a lack of immune system, tumor microenvironment composed of different cell types, and blood vessels. Further, the nutrient and hypoxia gradient that naturally arise in the spheroids do not resemble the more intricate heterogeneity present *in vivo*. We do, however, believe that *in vitro* models play an important role and are crucial to underpin radiobiological principles,[56] and should be able to capture some of the fundamental characteristics of the mechanisms underlining the FLASH effect. Suggestively, the spheroid model may capture some characteristics of early tumor growth within areas of microscopic tumor infiltration. The $FaDu_{small\ hypoxia}$ were not monitored for the full 3 months, potentially biasing the results. The reported oxygen level only refers to the oxygen tension in the medium surrounding the spheroids. It is plausible to assume that the same oxygen tension applies for the outermost cells of the spheroid, whereas the inner core of the spheroid should have a lower tension. In the study, we had no methods to detect the oxygen level across the spheroids, other than immunofluorescence staining using hypoxia markers. Although the study provides evidence of an oxygen dependence for the sparing effect at UHDR, it does not provide evidence that oxygen depletion is the underlying mechanism.

To conclude, we have shown that the UHDR response in spheroids differs between cancer cell lines as well as within the same cancer cell line. Under certain conditions UHDR and CONV are iso-efficacious, but other spheroids are spared by UHDR. A reduction in the available oxygen induces a sparing effect. For the cancer cell lines studied, both proton-UHDR and electron-UHDR provided iso-efficacious results for small spheroids under ambient conditions. Further studies in tumor-specific factors affecting the UHDR response and their relationship to oxygen are warranted to map and understand the underlying mechanism of FLASH. Also, additional *in vivo*-studies using TCD_{50}-assays and a variety of cancer models under different conditions seem indicated.

Supplementary material

Supplementary material is available at *BJR* online.

Funding

This work was supported by the Swedish Society for Medical Research (SSMF, grant 23-0341), Mrs. Berta Kamprad's Cancer Foundation (grant 2022-31-406), Swedish Cancer Society (grant 20 1298 Pj 01 H, 21 1929 S 01 H, and 24 3507 Pj 01 H), Gunnar Nilsson Cancer Foundation, and Swedish Governmental Funding for Clinical Research (ALF).

Conflicts of interest

None declared.

References

1. Favaudon V, Caplier L, Monceau V, et al. Ultrahigh dose-rate FLASH irradiation increases the differential response between normal and tumor tissue in mice. *Sci Transl Med*. 2014; 6:245ra93.
2. Montay-Gruel P, Acharya MM, Petersson K, et al. Long-term neurocognitive benefits of FLASH radiotherapy driven by reduced reactive oxygen species. *Proc Natl Acad Sci USA*. 2019; 116:10943-10951.
3. Velalopoulou A, Karagounis I V., Cramer GM, et al. Flash proton radiotherapy spares normal epithelial and mesenchymal tissues while preserving sarcoma response. *Cancer Res*. 2021; 81:4808-4821.
4. Sørensen BS, Kanouta E, Ankjærgaard C, et al. Proton FLASH: impact of dose rate and split dose on acute skin toxicity in a murine model. *Int J Radiat Oncol Biol Phys*. 2024; 120:265-275.
5. Böhlen TT, Germond J-F, Petersson K, et al. Effect of conventional and ultrahigh dose rate FLASH irradiations on preclinical tumor models: a systematic analysis. *Int J Radiat Oncol Biol Phys*.2023; 117:1007-1017.
6. Sørensen BS, Sitarz MK, Ankjærgaard C, et al. Pencil beam scanning proton FLASH maintains tumor control while normal tissue damage is reduced in a mouse model. *Radiother Oncol*. 2022; 175:178-184.
7. Munro TR, Gilbert CW. The relation between tumour lethal doses and the radiosensitivity of tumour cells. *Br J Radiol*. 1961; 34:246-251.
8. Kummer B, Löck S, Gurtner K, et al. Value of functional in-vivo endpoints in preclinical radiation research. *Radiother Oncol*. 2021; 158:155-161.
9. Budach W, Budach V, Stuschke M, et al. The TCD50 and regrowth delay assay in human tumor xenografts: differences and implications. *Int J Radiat Oncol Biol Phys*. 1993; 25:259-268.
10. Suit HD, Howes AE, Hunter N. Dependence of response of a C3H mammary carcinoma to fractionated irradiation on fractionation number and intertreatment interval. *Radiat Res*. 1977; 72:440-454.
11. Milas L, Yamada S, Hunter N, et al. Changes in TCD50 as a measure of clonogen doubling time in irradiated and unirradiated tumors. *Int J Radiat Oncol Biol Phys*. 1991; 21:1195-1202.
12. du Sert NP, Hurst V, Ahluwalia A, et al. The arrive guidelines 2.0: updated guidelines for reporting animal research. *PLoS Biol*. 2020; 18:1-12.
13. Workman P, Aboagye EO, Balkwill F, et al. Guidelines for the welfare and use of animals in cancer research. *Br J Cancer*. 2010; 102:1555-1557.
14. Sunnerberg JP, Tavakkoli AD, Petusseau AF, et al. Oxygen consumption *in vivo* by ultra-high dose rate electron irradiation depends upon baseline tissue oxygenation. *Int J Radiat Oncol Biol Phys*. 2025; 121:1053-1062.

15. Scarmelotto A, Delprat V, Michiels C, et al. The oxygen puzzle in FLASH radiotherapy: a comprehensive review and experimental outlook. *Clin Transl Radiat Oncol*. 2024; 49:100860. doi: 10.1016/j.ctro.2024.100860.
16. Grilj V, Leavitt RJ, El Khatib M, et al. *In vivo* measurements of change in tissue oxygen level during irradiation reveal novel dose rate dependence. *Radiother Oncol*. 2024; 201:110539.
17. Leavitt RJ, Almeida A, Grilj V, et al. Acute hypoxia does not alter tumor sensitivity to FLASH radiation therapy. *Int J Radiat Oncol Biol Phys*. 2024; 119:1493-1505.
18. Zhang Q, Gerweck LE, Cascio E, et al. Proton FLASH effects on mouse skin at different oxygen tensions. *Phys Med Biol*. 2023; 68:055010.
19. Adrian G, Konradsson E, Lempart M, et al. The FLASH effect depends on oxygen concentration. *Br J Radiol* 2020; 93:20190702.
20. Böhlen TT, Germond J-F, Bourhis J, et al. Normal tissue sparing by FLASH as a function of single-fraction dose: a quantitative analysis. *Int J Radiat Oncol Biol Phys*. 2022; 145:1032-1044.
21. Chabi S, To TH Van, Leavitt R, et al. Ultra-high-dose-rate FLASH and conventional-dose-rate irradiation differentially affect human acute lymphoblastic leukemia and normal hematopoiesis. *Int J Radiat Oncol Biol Phys*. 2021; 109:819-829.
22. Adrian G, Konradsson E, Beyer S, et al. Cancer cells can exhibit a sparing FLASH effect at low doses under normoxic in vitro-conditions. *Front Oncol* 2021; 11:1-9.
23. Montay-Gruel P, Corde S, Laissue JA, Bazalova-Carter M. FLASH radiotherapy with photon beams. *Med Phys*. 2021; 148:148-162.
24. Kristensen L, Rohrer S, Hoffmann L, et al. Electron vs proton FLASH radiation on murine skin toxicity. *Radiother Oncol*. 2025; 206:110796.
25. Almeida A, Togno M, Ballesteros-Zebadua P, et al. Dosimetric and biologic intercomparison between electron and proton FLASH beams. *Radiother Oncol*. 2024; 190:109953.
26. Kacem H, Psoroulas S, Boivin G, et al. Comparing radiolytic production of H2O2 and development of Zebrafish embryos after ultra high dose rate exposure with electron and transmission proton beams. *Radiother Oncol*. 2022; 175:197-202.
27. Murphy RJ, Gunasingh G, Haass NK, Simpson MJ. Growth and adaptation mechanisms of tumour spheroids with time-dependent oxygen availability. *PLoS Comput Biol*. 2023; 19:1-29.
28. Friedrich J, Ebner R, Kunz-Schughart LA. Experimental anti-tumor therapy in 3-D: spheroids—old hat or new challenge? *Int J Radiat Biol*. 2007; 83:849-871.
29. Lempart M, Blad B, Adrian G, et al. Modifying a clinical linear accelerator for delivery of ultra-high dose rate irradiation. *Radiother Oncol* 2019; 139:40–5.
30. Konradsson E, Wahlqvist P, Thoft A, et al. Beam control system and output fine-tuning for safe and precise delivery of FLASH radiotherapy at a clinical linear accelerator. *Front Oncol* 2024; 14:1–11.
31. Kanouta E, Poulsen PR, Kertzscher G, et al. Time-resolved dose rate measurements in pencil beam scanning proton FLASH therapy with a fiber-coupled scintillator detector system. *Med Phys* 2023; 50:2450–62.
32. Levy K, Natarajan S, Wang J, et al. Abdominal FLASH irradiation reduces radiation-induced gastrointestinal toxicity for the treatment of ovarian cancer in mice. *Sci Rep*. 2020; 10:21600.
33. Montay-Gruel P, Bouchet A, Jaccard M, et al. X-rays can trigger the FLASH effect: ultra-high dose-rate synchrotron light source prevents normal brain injury after whole brain irradiation in mice. *Radiother Oncol*. 2018; 129:582-588.
34. Fouillade C, Curras-Alonso S, Giuranno L, et al. FLASH irradiation spares lung progenitor cells and limits the incidence of radio-induced senescence. *Clin Cancer Res*. 2020; 26:1497-1506.
35. Montay-Gruel P, Petersson K, Jaccard M, et al. Irradiation in a flash: unique sparing of memory in mice after whole brain irradiation with dose rates above 100 Gy/s. *Radiother Oncol*. 2017; 124:365-369.
36. Browning AP, Sharp JA, Murphy RJ, et al. Quantitative analysis of tumour spheroid structure. *Elife* 2021; 10:1-25.
37. Adrian G, Ceberg C, Carneiro A, Ekblad L. Rescue effect inherited in colony formation assays affects radiation response. *Radiat Res*. 2018; 189:44-52.
38. Gupta N, Lamborn K, Deen DF. A statistical approach for analyzing clonogenic survival data. *Radiat Res*. 1996; 145:636-640.
39. Pomp J, Wike JL, Ouwerkerk IJM, et al. Cell density dependent plating efficiency affects outcome and interpretation of colony forming assays. *Radiother Oncol*. 1996; 40:121-125.
40. Tinganelli W, Weber U, Puspitasari A, et al. FLASH with carbon ions: tumor control, normal tissue sparing, and distal metastasis in a mouse osteosarcoma model. *Radiother Oncol*. 2022; 175:185-190.
41. Konradsson E, Liljedahl E, Gustafsson E, et al. Comparable long-term tumor control for hypofractionated FLASH *vs*. conventional radiation therapy in an immunocompetent rat glioma model. *Adv Radiat Oncol* 2022;7: 101011.
42. Bourhis J, Montay-Gruel P, Gonçalves Jorge P, et al. Clinical translation of FLASH radiotherapy: why and how? *Radiother Oncol*. 2019; 139:11-17.
43. Eggold JT, Chow S, Melemenidis S, et al. Abdominopelvic FLASH irradiation improves PD-1 immune checkpoint inhibition in preclinical models of ovarian cancer. *Mol Cancer Ther*. 2022; 21:371-381.
44. Diffenderfer ES, Verginadis II, Kim MM, et al. Design, implementation, and *in vivo* validation of a novel proton FLASH radiation therapy system. *Int J Radiat Oncol Biol Phys*. 2020; 106:440-448.
45. Kim YE, Gwak SH, Hong BJ, et al. Effects of ultra-high doserate FLASH irradiation on the tumor microenvironment in lewis lung carcinoma: role of myosin light chain. *Int J Radiat Oncol Biol Phys*. 2020; 109:1440-1453.
46. Montay-Gruel P, Acharya MM, Gonçalves Jorge P, et al. Hypofractionated FLASH-RT as an effective treatment against glioblastoma that reduces neurocognitive side effects in mice. *Clin Cancer Res*. 2021; 27:775-784.
47. Liljedahl E, Konradsson E, Linderfalk K, et al. Comparable survival in rats with intracranial glioblastoma irradiated with single-fraction conventional radiotherapy or FLASH radiotherapy. *Front Oncol*. 2024; 13:1-10.
48. Liljedahl E, Konradsson E, Gustafsson E, et al. Long-term anti-tumor effects following both conventional radiotherapy and FLASH in fully immunocompetent animals with glioblastoma. *Sci Rep*. 2022; 12:12285.
49. Khan S, Bassenne M, Wang J, et al. Multicellular spheroids as *in vitro* models of oxygen depletion during FLASH irradiation. *Int J Radiat Oncol Biol Phys*. 2021; 110:833-844.
50. Shibamoto Y, Yukawa Y, Tsutsui K, et al. Variation in the hypoxic fraction among mouse tumors of different types, sizes, and sites. *Jpn J Cancer Res*. 1986; 77:908-915.
51. Baumann M, Krause M, Zips D, et al. Selective inhibition of the epidermal growth factor receptor tyrosine kinase by BIBX1382BS and the improvement of growth delay, but not local control, after fractionated irradiation in human FaDu squamous cell carcinoma in the nude mouse. *Int J Radiat Biol* 2003; 79:547-559.
52. McNally NJ, Sheldon PW. The effect of radiation on tumour growth delay, cell survival and cure of the animal using a single tumour system. *Br J Radiol*. 1977; 50:321-328.
53. Coleman CN, Higgins GS, Brown JM, et al. Improving the predictive value of preclinical studies in support of radiotherapy clinical trials. *Clin Cancer Res*. 2016; 22:3138-3147.
54. Liu K, Waldrop T, Aguilar E, et al. Redefining FLASH radiation therapy: the impact of mean dose rate and dose per pulse in the gastrointestinal tract. *Int J Radiat Oncol Biol Phys*. 2025; 121:1063-1076.
55. Kyle AH, Karan T, Baker JHE, et al. Detection of FLASH-radiotherapy tissue sparing in a 3D-spheroid model using DNA damage response markers. *Radiother Oncol*. 2024;196: 110326.
56. Adrian G, Ruan J, Paillas S, et al. *In vitro* assays for investigating the FLASH effect. *Expert Rev Mol Med*. 2022; 24:e10.

British Journal of Radiology, 2026, 99, 65–72
https://doi.org/10.1093/bjr/tqaf219
Research Article